

Experimental and Artificial Neural Networks Modeling for Rivers Bed Morphology Changes near Direct Water Supply Intakes

Rasul M. Khalaf¹ Rafa H. Al-Suhaili² Sanaa A. T. Al-Osmy³

1 Department of Civil Engineering, University of Al-Mustansiriyah, Baghdad, Iraq.

2 Department of Civil Engineering, University of Baghdad, Baghdad, Iraq.

Visiting Prof. , City College of New York. New York, USA.

3 Department of Civil Engineering, University of Al-Mustansiriyah, Baghdad, Iraq.

ABSTRACT

In this research, the problem of sediment movements near direct intakes was investigated from the river bed morphology point of view rather than that concerning the effect of sediment withdrawal by the intake to the water treatment plant. As expected the river bed morphology will be affected by the intake operation, and when the pumping stops, the river will tend to recover this effect by its natural flow, hence a model is required to relate the rate of river bed morphology recovery to the variables that are expected to be relevant, such as the pumping rate, the geometrical variables and time of operation to time of non-operation ratio. A physical model was built. Experiments were conducted to create a data base for these input-output variables, which were used to find an (ANN) model, for the representation of this relationship. Image processing technique is used in this study to analyze the scour and deposition photos from which the volumes of the scour holes after intake operation time and that after intake non-operation time were found, which allows the estimation of the rate of recovery. The results obtained from the image processing of these photos had prevailed that these volumes can be approximated as a half ellipsoid. An ANN.-factorized back propagation model was fitted to the data base with a correlation coefficient of (0.843), which was considered acceptable according to Smith (1986) criteria. Comparison between the output values(rate of recovery) obtained using this (ANN) model and those obtained experimentally for cases that are not included in the data base, indicates high compatibility with a maximum percentage difference of (7.15% and 5.07%) for overestimating and underestimating respectively.

Keywords: River morphology, Souring, Sedimentation, Rate of recovery, Artificial Neural Networks, Water intakes.

I. INTRODUCTION

Sediment movement near the river intake structures is a complex problem that reduces the system efficiency and increases the cost of dredging and system maintenance. In case of power-plants using river-cooling water, sediment reduces the withdrawn capacity of the plant, causes damage to the pumping system and partial or full blockage at the entrance of intake. Sediment blockage may result in the stopping of the plant, Abd Al-Haleem, (2008).

As water is abstracted through the intake, sediment is typically drawn towards the intake structure or point of diversion. Sediment may either be drawn into the intake structure or may be trapped behind it. This reduces the amount of sediment that is supplied to downstream reaches. If sediment is drawn into the intake, there is the risk of damage to the intake facility and end operation machinery (e.g. turbines, gates and valves), Ali et al.(2012).

Many researches had been conducted concerning the problem that occurs in the water supply projects due to sediment withdrawal, Amin (2005),Zheng and Alsaffar(2000). However, very little work had been done on the effect of direct water intakes operation on the river bed morphology, Formann et al. (2012), Zaitsev et al.(2004). These intakes operation can affect the river bed morphology by creating considerable changes in the bed formation near the intake, and disturb the river as a system. This operation causes movement of sediments near the intake creating some sort of a hole in the vicinity of the intake. Part of the sediments moved due to pumping will be withdrawn with the pumped water, while the other part will move just downstream the intake where it deposited creating local sediment accumulation. The reduction in sediment downstream and increased erosion can damage important habitats (e.g. bank-side habitat) and habitats

that depend on a supply of sediment from upstream reaches, SEPA (2008).

For a scientific and rational approach to different river problems and proper planning and design of water resources projects, an understanding of the morphology and behavior of the river is a pre-requisite. River morphology is a field of science which deals with the change of river plan and cross sections due to sedimentation and erosion. In this field, dynamics of flow and sediment transport are the principal elements. The morphological studies, therefore, play an important role in planning, designing and maintaining river engineering structures, Agrawl(2005).

These changes in the river morphology near the intake may disturb the natural river system. It may have effects on the natural flow and the ecosystem. However, the river system will try to retain its natural properties when the disturbance created by the water intake operation stop. This is the recovery property of any natural system such as rivers.

Artificial neural networks modeling had been used for the modeling of scour phenomena at outlet structures, Emamgholizadeh (2012). These models had proved their capability of estimating the depth of scour holes created by the flow around bridge piers, Jeng et al. (2005).

In this research it is intended to look at the problem of sediment movements near direct intakes from the river bed morphology point of view rather than those problems concerning the water treatment. The reasons for this attention are due to the facts that little researches had been conducted on this issue compared to the concern of the water treatment problems, and that so many direct intakes were already exist in Iraq and still working. Exchanging these direct intakes into side intakes is an expensive and impractical action, hence it is believed that proper operation of these direct intakes can minimize the effect on the river morphology.

The following main steps were conducted to achieve the aim of the research.

- 1- Building a physical model, that simulates a direct intake operation on a river.
- 2- Conduct experiments to establish a data base for the set of data relating the rate of recovery of the river bed material to the pumping rate and time schedule.

- 3- 3- Develop an artificial neural networks model for relating the variables using the data base developed in step2.

II. THE EXPERIMENTAL SETUP

A movable bed flume, re-circulating type was built. Its parts are collected from different public markets in Baghdad, Iraq, such as electrical pumps and flow meters. The system is a closed operating system. Figure (1) shows the general layout of the flume. The flume is consisted of the following main parts:

Flume Body

The main flume is of 3m long and has a rectangular cross-section (1.2 m x 1 m). The flume structure is built up from iron and its sides and bed are manufactured from 8 mm thickness acrylic material, The entrance of the flume is provided with a stilling basin with a fine mesh screen to ensure an even flow distribution across the flume. At the downstream end of the flume, there exists a rectangular Sharp crested weir which has been manufactured to calculate the flume (river) flow. The working section of the flume is 2.5m length, 1.2m width and 1m in depth. This working section is filled with 15cm thickness layer of natural river soil taken from Tigris River.

Ground Tank with Re-circulating Pump

The ground tank was built using aluminum material, has dimensions of (3 m x 1.20 m x 2 m). Water is pumped from this tank to the flume, by means of two centrifugal pumps each with a capacity of (280) lit/s. The suction pipe of the centrifugal pump is (3) m long and (0.33) m in diameter. It is submerged in the ground tank to deliver water for the flume. Figure (2) shows the ground tank and the re-circulating pump.

Intake Structure

The intake structure is made up of a suction pump with a capacity of (500) lit/sec which was used to withdraw water from the flume through the intake pipe to the storage or ground tank. This pump is connected with a UPVC pipe (1.25)" ,in diameter and (40)" ,in length which works as an intake vertical pipe. This pipe was submerged into the river (flume) and convey the water to the flume (river) then finally to the ground tank as shown in figure (3).

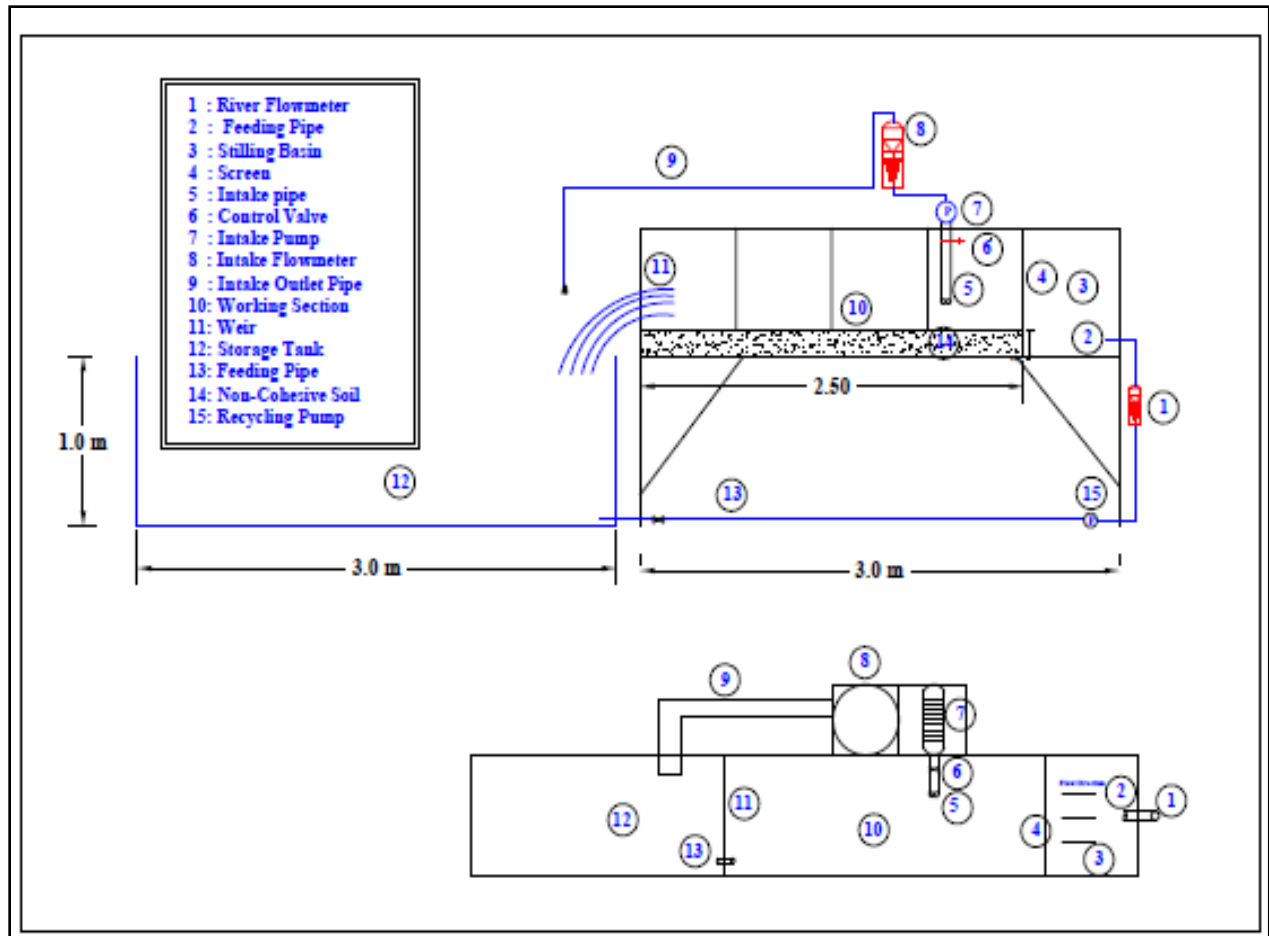


Fig. (1) General layout of the flume



Fig.(2) Ground water storage tank and re-circulating pumps.

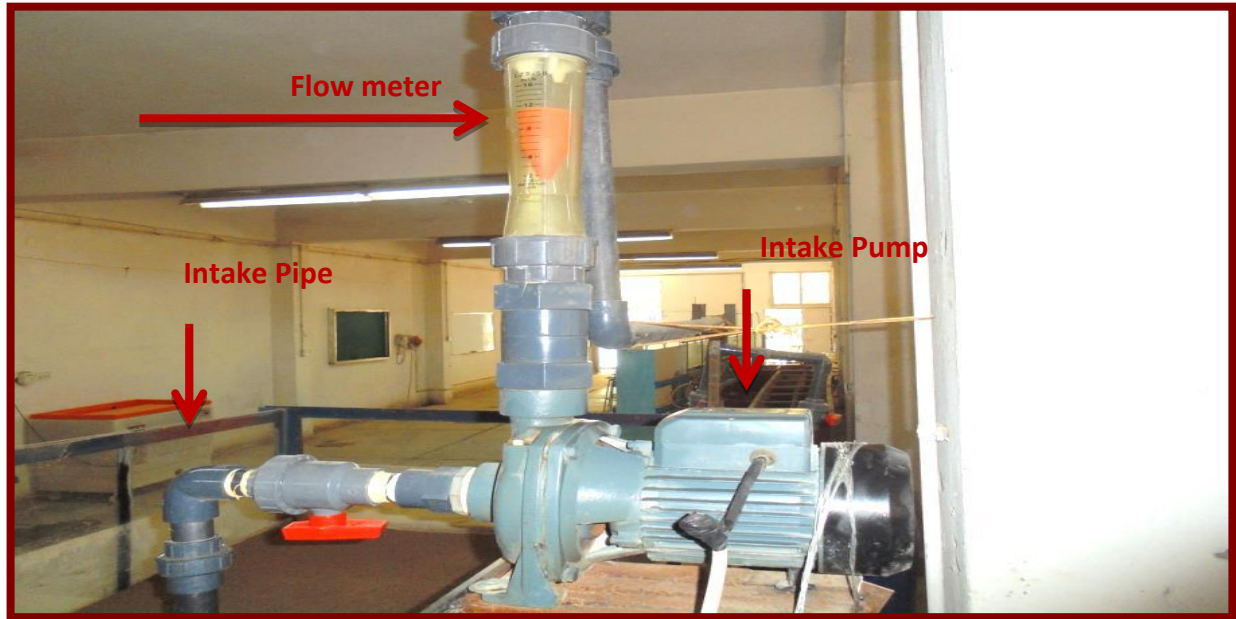


Fig. (3) Intake pump and flowmeter.

Flow meters

The inlet flow to the flume and outlet flow from the intake pump were measured by using two flow meters. One of them is connected to the flume

inlet pipe which was coming from the ground pumps to measure the flume flow (QR) and the other is connected to the intake pump to measure the intake flow as shown in figure (4).



Fig. (4) Ground flow meter and intake flow meter for measuring the intake discharge.

Point gauge

A Point gauge was installed within the flume as shown in figure (5). A Carriage was constructed on the two rails on the two sides of the main and intake flumes. The carriage could be moved along the whole length of the flume. The point gauge was fitted on the

carriage and used to measure both water and bed levels. An industrial scraper was manufactured from an iron material in order to be used for making a level bed before each run. The point gauge was also used to measure the bed topography on the working section of the flume before each run.



Fig. (5) The movable point gauge.

Digital Camera

A digital camera of (16Mega Pixel) was used to monitor the bed topography on the whole working section (2.5)m with a grid of (60 cm x 60 cm) around the intake suction pipe. The photos were then analyzed by using the image processing technique.

III. EXPERIMENTAL PROGRAM

Experiments were carried out considering the main parameters that affect the movement of the non-cohesive sediments near the water intakes. The studied effective parameters are as follows:-

- intake pumping flow, (Q_p)
- River flow, (Q_R)
- horizontal position of the intake pipe, (d)
- width of the river(flume), (w)
- horizontal coordinate of any point along the river flow direction, (x)
- length of river reach, (L_r)
- Transverse coordinate of any point along the direction perpendicular to river flow direction (along the tank width direction), (y)
- depth of sediments at any point (x, y), (z)
- Vertical position of the intake point, (d_{sn})
- Normal depth of river, (Y_n)
- time of operation condition of the intake, t_{op}
- time of non-operation condition of the intake, t_{nop}

The experimental tests are divided into many different sets. For each set of experiments, different ratios of (Q_r) i.e., (Q_p/Q_r) were used. For each value of discharge ratio, different values of time ratios (t_r) i.e., (t_{op}/t_{nop}) were used.

IV. EXPERIMENTAL RESULTS ANALYSIS

The analysis of the experimental results is presented here for some of the experiments only for the purpose of illustration. The given sample will show the obtained scour hole after direct pumping and the analysis of its photo using the image processing technique. The recovery of scour hole after non-operating stage is also shown here using the image processing technique. Figure (6) shows a typical scour hole photo and its image processing analysis. Figures (7) and (8) show the scour hole and its image processing before and after operation of the intake for $Q_r=0.37, t_r=0.33$, the estimated percentage recovery is $Pr=82.69\%$. All the photos of the other experimental work runs were analyzed in a similar manner to that shown in figures (7) and (8), using the image processing technique. This technique can give the dimensions of the scour hole after operation and non-operation periods. The image processing technique can also give the z - coordinate for the (x - y) coordinates of any point on the scour hole. It also can draw a section of the z - coordinates along any longitudinal line (x), and/or transverse line (y), selected through the scour hole section. For each photo of scour hole, relation between x - y coordinates and depth z can be obtained through the scour section. Table (1) represents the depths (z) at different locations in a rectangular section (60*60)cm, i.e., the z - coordinates for each 6 cm along x and y directions of the section, for one of the images analyzed.

Investigating all of the experimental results had revealed that the shape of scour hole is similar to a half of an ellipsoid, hence the volume of scour hole can be approximated by the following formula:

$$V = \frac{1}{2} * \frac{2}{3} \pi \cdot L_{S1} \cdot L_{S2} \cdot ds \quad (1)$$

Where:

L_{S1} =Horizontal axis of the ellipsoid.

L_{S2} =Vertical axis of the ellipsoid.

ds = central depth of scour hole.

Table (2) represents the obtained experimental results for some experiments conducted. These data can be classified into two parts:

- 1- The data which were measured during the experiments such as (Y_n , ds_n , Q_p , Q_r , t_{op} and t_{nop}).
- 2- The data obtained from the image processing analysis of the scour holes volumes after pumping operating and non-operating periods, (V_{op} , V_{nop} and $Pr\%$), which are the volume of hole after the operation of intake, volume of hole after the period of non-operation of the intake, and the percent recovery of the hole, respectively. The percentage recovery is estimated using the following equation:

$$Pr = \frac{V_{op} - V_{nop}}{V_{op}} * 100 \quad (2)$$

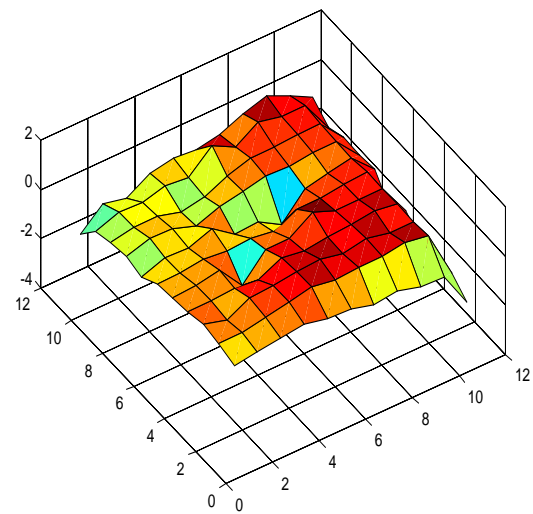


Fig. (6) A sample of a scour hole photo and its image processing after pumping operation time.



A)



B)

Fig. (7) A scour hole photos for ($Q_r=0.37$, $t_r=0.33$, $PR=82.69\%$), A) after pumping operation time period, B) after non operation time period.

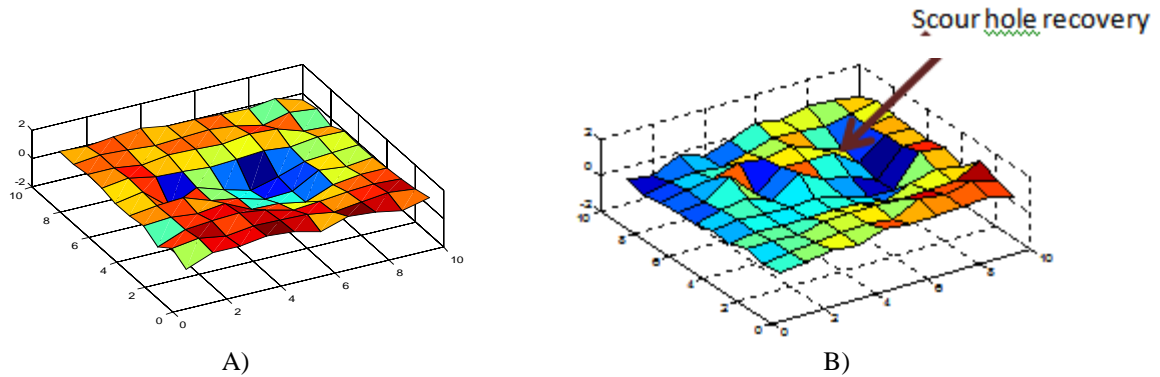


Fig. (8) Image Processing for the Scour holes for ($Q_r=0.37, t_r=0.33$, $PR=82.69\%$), A) after pumping operation time period, B) after non operation time period.

Table(1) Sample of the Image Processing Data results for a sample run.

X Y	1	2	3	4	5	6	7	8	9	10
1	0.921	-0.275	-0.082	0.303	-0.506	-0.159	-0.005	-0.622	0.072	-0.198
2	0.033	-0.043	-0.159	-0.082	-0.005	-0.236	0.535	-0.506	-0.699	0.226
3	0.303	0.342	0.998	0.342	-0.043	0.110	-0.468	-0.120	0.188	0.265
4	0.265	-0.120	1.114	-0.082	0.767	-1.085	0.381	-0.275	0.574	-0.005
5	0.419	0.265	0.805	0.535	-1.664	-0.854	-0.120	0.303	0.612	0.381
6	0.496	0.728	0.265	-0.429	-1.626	-0.159	0.033	0.072	0.458	0.188
7	-0.352	0.651	0.805	-0.236	-0.468	0.072	0.496	0.689	0.419	-0.082
8	0.651	0.728	0.458	0.342	0.149	-0.622	0.767	0.072	-1.047	0.728
9	0.033	0.574	0.921	0.033	0.188	-0.005	0.612	-0.545	0.188	0.149
10	-0.468	-1.047	-0.54	-0.429	-0.198	0.265	-0.159	-1.008	-0.506	-0.506

Table (2) Sample of the measured experimental results.

Run No.	Q_p (m^3/sec)	Q_r (m^3/sec)	d (cm)	W (cm.)	dsn (cm.)	Y_n (cm.)	top (min.)	tnop (min.)
1	4.1	5.83	32	120	18	22	9	25
2	3.35	5.8	32	120	21	22.5	9	20
3	3.53	6.33	29	120	16	19	13.5	40
4	3.19	7.614	27.5	120	14.5	17.5	27	50
5	3.19	4.68	27.5	120	10.5	14.5	15	30
6	2.91	3.86	34	120	13.5	17.2	33	60
7	3.05	4.76	34	120	14.2	18.2	25	90
8	2.23	2.84	34	120	13.3	18.3	21	35

9	2.18	4.33	34	120	15.8	19.8	18	60
10	2.79	4.53	34	120	16.2	18.2	9	31
11	3.19	5.61	34	120	18.5	20	13	40
12	3.48	4.53	34	120	17	19	10	60
13	2.31	3.19	34	120	19	22	10.5	41

The Developed ANN Model

Using the data base developed in the experimental work and ANN modeling technique, different trials were made and finally an ANN-factorized back propagation model was obtained with a correlation coefficient of (0.843), which was considered acceptable according to smith(1986) criteria. The input variables were changed to a dimensionless terms to provide generality of the model. These dimensionless variables are as follows:
 $dow=(d/w)$, the ratio of the horizontal position of the intake pipe to the river width.
 $Qr=(Qp/QR)$, the ratio of the pumped discharges to the river discharge.
 $tr=(top/tnop)$, the ratio of the time of operation of the intake to time of non-operation.

$dr=(dsn/yn)$, the ratio of the depth of the submergence of the intake strainer to the normal depth of the river.

These variables were used as input variables, while the rate of recovery Pr is used as the output variable. The SPSS (Statistical Procedures of Social Sciences), version 19 was used for obtaining the required ANN model.

Table (3) shows the data division, where the application of (SPSS) software allows the selection of this data division into training set, testing set, and validation (holdout) set. The best data division that was obtained is 79.2% (38Runs) for training, 8.3% (4 Runs) for testing, and 12.5% (6 Runs) for the validation.

Table(3) Case Processing Summary.

		N	Percent %
Sample	Training	38	79.2
	Testing	4	8.3
	Holdout	6	12.5
Valid		48	100
Excluded		0	
Total		48	

Table (4) shows the model network information, which indicates a number of hidden nodes in the hidden layer of (7). The obtained required activation functions for the hidden and output layers were hyperbolic tangent and identity functions respectively. Figure (9) shows the architecture of the network.

Table (4) Artificial neural network information.

Input Layer	Factors	1	dow
	Covariates	1	Qr
		2	tr
		3	dsn/yn
	Number of Units*	9	
Rescaling Method for Covariates		Standardized	
Hidden Layer(s)	Number of Hidden Layers	1	

Output Layer	Number of Units in Hidden Layer 1*	7
	Activation Function	Hyperbolic tangent
	Dependent Variables	1
	Number of Units	1
	Rescaling Method for Scale Dependents	Standardized
	Activation Function	Identity
	Error Function	Sum of Squares

*. Excluding the bias unit

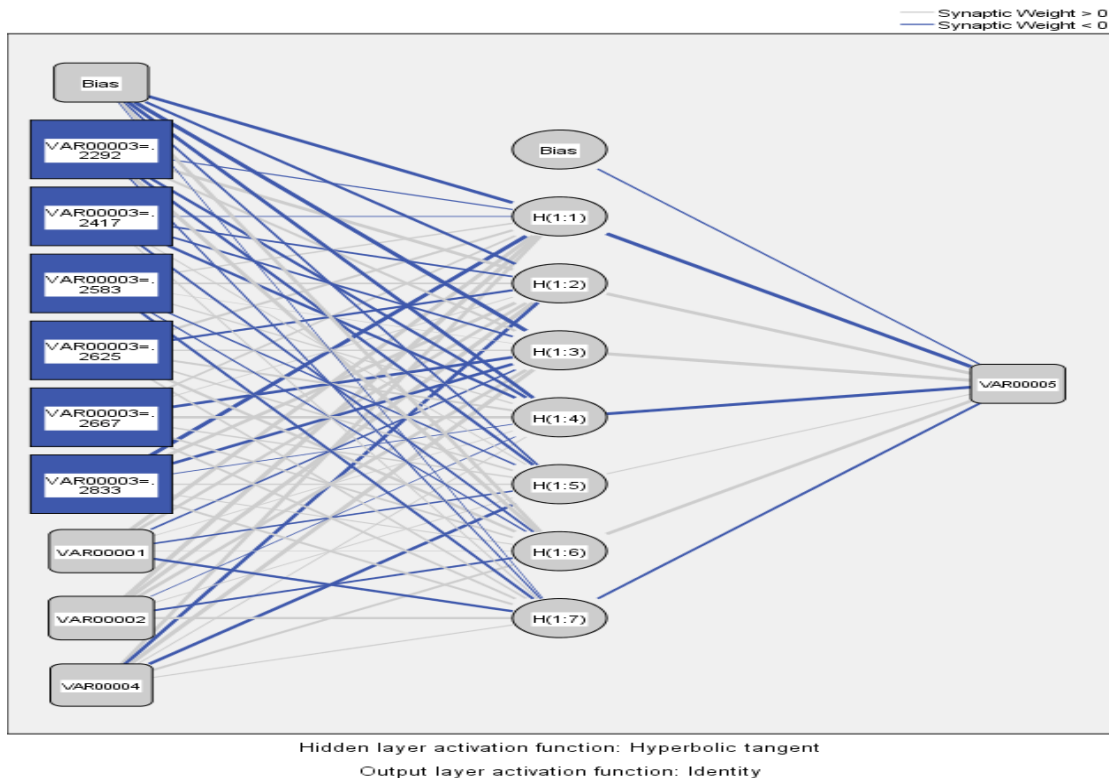


Figure (9) The architecture of the artificial neural network (ANN) model required for the modeling of the phenomena.

Table(5) shows the error analysis of the obtained ANN model. This table indicates low sum of square errors and relative errors for each of the training, testing and verification subsets.

Table (5) Error analysis of the developed ANN model.

Training	Sum of Squares Error	3.654
	Relative Error	0.197
	Stopping Rule Used	1 consecutive step(s) with no decrease in error*
	Training Time	0:00:00.03
Testing	Sum of Squares Error	1.620
	Relative Error	1.079
Holdout	Relative Error	2.462

Dependent Variable: Pr

*. Error computations are based on the testing sample.

Table (6) shows the model parameters vectors and matrices obtained for the model. The correlation coefficient between the predicted and measured percentage recovery is (0.843).

Table (6) The ANN model Parameters.

Predictor		Predicted							Output Layer
		Hidden Layer 1							
		H(1:1)	H(1:2)	H(1:3)	H(1:4)	H(1:5)	H(1:6)	H(1:7)	
Input Layer	(Bias)	-0.930	-0.548	-1.398	-0.766	-0.220	0.656	-0.023	
	[VAR00003= 2292]	-0.096	0.956	0.487	-0.546	-0.514	0.862	-0.098	
	[VAR00003= 2417]	-0.045	-0.337	-0.339	-0.615	0.063	-0.266	0.078	
	[VAR00003= 2583]	0.182	0.310	0.021	0.108	-0.174	-0.101	-0.397	
	[VAR00003= 2625]	0.501	-0.527	0.120	0.455	0.244	0.574	0.199	
	[VAR00003= 2667]	0.252	0.041	-0.874	0.770	0.195	0.318	0.347	
	[VAR00003= 2833]	-1.287	0.886	-0.766	-0.036	0.146	0.073	0.385	
	VAR00001	0.969	0.644	-0.197	0.033	-0.229	0.023	-0.551	
	VAR00002	1.498	1.159	0.693	-0.031	0.042	-0.375	0.532	
VAR00004	0.677	-0.658	1.105	0.053	-0.743	0.469	0.095		
Hidden Layer 1	(Bias)								-1.17-
	H(1:1)								-1.389-
	H(1:2)								1.037
	H(1:3)								1.591
	H(1:4)								-1.026-
	H(1:5)								0.67
	H(1:6)								0.849
	H(1:7)								-0.378-

In order to use the developed ANN model for estimating the rate of recovery for a given input data set the model can be represented by the following steps:

- Put the input variables (dow, Qr, tr and dsn/yn) in a the input vector X_i and obtain a standardized form column vector $X_{n,1}^*$ using the following equation:

$$X_i^* = \frac{X_i - \text{mean}x_i}{Sdx_i} \quad (3)$$

Where: X_i^* , and X_i are the standardized and normal input variables respectively, $i=1,2,\dots,N$, where N is the number of input variables (N=4 for the developed model), and $\text{mean}x_i, Sdx_i$ are the observed means and standard deviations of the input variables.

- Obtain the weighted input vector to the nodes of the hidden layer $Zin_{p,1}$, using the following matrix equation:

$$Zin_{p,1} = Vobias_{p,1} + V_{n,p}^T * X_{n,1}^* \quad (4)$$

Where: $Vobias_{p,1}$, and $V_{n,p}$ are the bias vector and weight matrix between the input and hidden layers, p is the number of hidden nodes in the hidden layer. For the developed model, p=7 and the vector and matrix are as given below:

$$Vobias_{p,1} = Vobias_{7,1} = \begin{pmatrix} -0.93 \\ -0.548 \\ -1.398 \\ -0.766 \\ -0.220 \\ 0.656 \\ -0.023 \end{pmatrix} \quad \dots (5)$$

$$V_{n,p} = V_{4,7} = \begin{pmatrix} 0.969 & 0.644 & -0.197 & 0.033 & -0.229 & 0.023 & -0.551 \\ 1.498 & 1.159 & 0.693 & 0.031 & 0.042 & -0.375 & 0.532 \\ a(1) & a(2) & a(3) & a(4) & a(5) & a(6) & a(7) \\ 0.677 & -0.658 & 1.105 & 0.053 & -0.743 & 0.469 & 0.095 \end{pmatrix} \quad (6)$$

Where the vector a(i), i=1 to 7 is given by table(7).

Table(7) Values of (a_i) vector related to (d/w) values.

d/w	a ₁	a ₂	a ₃	a ₄	a ₅	a ₆	a ₇
0.2292	-0.096	0.956	0.487	-0.456	-0.517	0.862	-0.098
0.2417	-0.045	-0.337	-0.339	-0.615	0.063	-0.266	0.078
0.2583	0.182	0.310	0.021	0.108	-0.174	-0.101	-0.397
0.2625	0.501	-0.527	0.120	0.455	0.244	0.574	0.199
0.2667	0.252	0.041	-0.874	0.770	0.195	0.318	0.347
0.2833	-1.287	0.886	-0.766	-0.036	0.146	0.073	0.385

3- Obtain the output vector from the nodes of the hidden layer as follows:

$$Zout_{p,1} = Fh(Zin_{p,1}) \quad (7)$$

Where: Fh is the activation function of the hidden layer. This function for the developed model is a hyperbolic tangent.

4- Obtain the input weighted vector to the nodes of the output layer, $Yin_{m,1}$ using:

$$Yin_{m,1} = Wobias_{m,1} + W_{p,m}^T * Zout_{p,1} \quad (8)$$

Where: $Wobias_{m,1}$, and $W_{p,m}$ are the bias vector and weight matrix between the hidden and output layers, m is the number of nodes in the output layer. For the developed model, m=1 and the vector and matrix are as given below:

$$Wobias_{m,1} = Wobias_{1,1} = (-0.117) \quad (9)$$

$$W_{p,m} = W_{7,1} = \begin{pmatrix} -1.389 \\ 1.037 \\ 1.591 \\ -1.026 \\ 0.067 \\ 0.849 \\ -0.378 \end{pmatrix} \quad (10)$$

5- Find the standardized output vector $Yout_{m,1}^*$

$$Yout_{m,1}^* = Fo(Yin)_{m,1} \quad (11)$$

and then obtain the output variables using:

$$Y_{j,1} = Y_{j,1}^* * Sdy_{mj} + meany_j \quad (12)$$

Where $j=1,2,...,m$. For the developed the output variable is only one, since $m=1$, and that is the value of Pr.

The reason for using the standardized variables in the ANN model as shown in equations (3) and (12) is that the model vectors and matrices parameters are estimated using the standardized input and output variables. This is usually recommended for ANN modeling to avoid the effect of order of magnitude of each variable on these parameters. However the SPSS software allows four method of modeling for the input variables, non-scaling, standardized, normalized and adjusted normalized. The standardized scaling method was used for the input data since it was found to produce the higher correlation coefficient between the

predicted and observed output variable. For the output variables, the software uses a standardization method by default, i.e. the output values (Pr%) is not the real values but the standardized values, hence using this model, the output values should be returned to the real values by multiplying by the standard deviation and adding the mean of each output variables. This will require also the calculation of a mean value and the standard deviation (sd) for output variable (Pr%) which will be used later for returning the real output values of (Pr%).

The mean and standard deviation values are needed for the model use as mentioned above, hence, considered as a model parameters. Table (8) shows these means and standard deviations.

Table (8) The means and standard deviations of the input-output variables.

Variable	Qr	tr	d/w	dsn/Yn	Pr
Mean	0.617143	0.319061	0.26399	0.892245	62.6795
Standard deviation	0.142285	0.13545	0.014037	0.047778	16.44976

Even though the ANN modeling process involves the division of data into three sub-samples as mentioned above, the training, testing and verification sub samples, and obtaining the model parameters using the first two sub-samples leaving the third sub-sample for verification, further verification was made herein to ensure the model performance. This further verification was done using some additional experimental data that

are not used in the ANN modeling. Table (9) shows the results of the observed and predicted rate of recovery of these additional experiments. The maximum percentage difference was found to be (7.15) overestimating and (5.07) underestimating. This ensures the model good performance. Hence this model can be used for design and/or operation purposes for direct intakes on rivers.

Designers and operators of such intake can use this model to estimate the rate of recovery for proposed or existing intake geometric and pumping capacity variables. For example if the required daily pumping volume is V and the proposed number of cycles per day is nc, then:

$$Top = \frac{V}{Q_p} \tag{13}$$

$$Top = nc (top + tnop) \tag{14}$$

$$tr = \frac{top}{tnop} \tag{15}$$

Table (9) Percentage difference between observed and estimated rate of recovery percent using the developed ANN model.

Input Variables				Output Variables		
Qr	tr	d/w	dsn/yn	PR Observed	PR Estimated	% difference
0.703	0.3600	0.2667	0.8182	73.5331	78.7900	-7.15
0.5577	0.3375	0.2417	0.8421	67.0000	70.1000	-4.69
0.7539	0.5500	0.2833	0.8430	54.2210	51.4700	5.07
0.7852	0.6000	0.2833	0.8361	40.1530	39.6300	1.30
0.7741	0.2561	0.2833	0.8636	89.8600	88.4140	1.62
0.7296	0.5000	0.2583	0.9444	77.2300	73.7900	4.46
0.5114	0.2500	0.2583	0.9000	63.3000	63.7900	-0.72

The designer and operators can use a trial and error procedure by the following steps:

- 1- For the given V and Q_p estimating Top from equation(13)
- 2- Solving equations(14) and (15) to find tr for a proposed values of nc and top.
- 3- Using the tr with the other proposed values as input variables in the developed ANN model to obtain the rate of recovery then repeating the process until a satisfied rate of recovery is obtained.

A relative normalized importance analysis was performed in order to find which of the input variables has the most effect on the output variable. Table (10) shows the results which indicate the effect of input variables in descending order as d/w, Qr, tr and ds/yn respectively. The last three variables has almost the same effect of approximately (60%) on the rate of recovery.

Table(8) Independent Variable Importance analysis.

Variable number	Variable name	Importance	Normalized importance
VAR00001	d/w	0.356	100%
VAR00002	Qr	0.216	60.7%
VAR00003	tr	0.219	61.6%
VAR00004	dsn/yn	0.209	58.71%

V. CONCLUSIONS:

Form the experimental and analytical study conducted above the following conclusions can be deduced:

- 1- Photos should be taken by fixing the digital camera at the same vertical location or level during the experimental work. Different locations of the camera will lead to different range of data and will not help to make a precise comparison between operation and non-operation behavior of

the river bed morphology. In addition to that photos should be taken using the same digital camera settings and the same section dimensions for all of the experiments. Using different pixels and section dimensions will lead to give different range of data, which will not give a real presentation of the phenomena under study.

- 2- The analysis of the results of the image processing indicate the possibility of approximating the volume of the created hole by measuring the

- principal axis of this hole and using the formula of half ellipsoid volume.
- 3- Comparison between the rates of recovery values obtained using the physical model with those obtained using the developed (ANN) model indicates high compatibility with a maximum percentage difference of (7.15% and 5.07%) for overestimating and underestimating respectively.
 - 4- The normalized importance analysis indicates that the ratio (d/w) has the highest effect on the rate of recovery with normalized relative importance of 100%.The other three variables (Qr, tr, dsn/yn) has almost the same normalized relative effect on the rate of recovery, which is about 60%.
 - 5- Using this modeling technique, different trials were made and finally an (ANN.-factorized back propagation model) was observed with a correlation coefficient of (0.843), which was considered acceptable according to smith criteria. The reason for obtaining a factorized ANN model rather than the traditional one is due to the fact that (d/w) was found to have an effect on the percent recovery as a factorized factor rather than as a variable.

Scour Depth Around Bridge Piers", Research Report No.R855, Department of Civil Engineering, University of Sydney, Australia, November 2005, <http://www.civil.usyd.edu.au/>.

- [7] Scottish Environment Protection Agency (SEPA), 2008, "Intakes And Outfalls" 1st Edition, October 2008.
- [8] Smith, M. (1993), "Neural Networks for Statistical Modeling", Van Nostrand-Reinhold, New York.
- [9] Zaitsev, A. A., Belikov, V.V. and Militeev, A. N. ,2004" Sediment Transfer Through the Fluvial System using Computer Modeling for Regulation of Sediment Transport Under Hydraulic Structures an A Large River ", Proceedings of A Symposium Held In Moscow, August 2004, IAHS Publ. 288, pp.386-394.
- [10] Zheng, Y. and Alsaffar, A. M. ,2000," Water Intake Sediment Problems in Thermal Power Plants", ASCE, Doi: 10.1061/40517(2000)273 ,pp. 1-8.

REFERENCES

- [1] Abd Al-Haleem, F.S.F., 2008,"Sediment Control At River Side Intakes", Ph.D Thesis, Department of Civil Engineering, Faculty of Engineering, Minufiya University ,Egypt.
- [2] Agrawal, A.K., 2005," Numerical Modeling of Sediment Flow In Tala Desilting Chamber" M. Sc. Thesis, Norwegian University of Science and Technology, Faculty of Engineering Science and Technology, Department of Hydraulic and Environmental Engineering, Norwig.
- [3] Ali, A. A., Al-Ansari N. A. and Knutsson, S. , 2012 , " Morphology of Tigris River Within Baghdad City", Journal of Hydrology and Earth System Sciences., 16, pp.3783–3790.
- [4] Amin, A. M. A. , 2005,"Study Of Sedimentation At River Side Intakes", Ph.D Thesis, Minufiya University, Faculty Of Engineering, Civil Engineering Department, Shebin El-Kom, Egypt.
- [5] Emamgholizadeh, S., 2012," Neural Network Modeling of Scour Cone Geometry Around Outlet in The Pressure Flushing", Global NEST Journal, Vol.14, No.4, pp. 540-549.
- [6] Jeng D-S, Bateni S. M., and Lockett E.,(2005)," Neural Network Assessment For